Proceedings of the
4th JSME-KSME Thermal Engineering Conference
October 1-6, 2000, Kobe, Japan

C207

# Study on Natural Convection in a Rectangular Enclosure with a Heating Source

**Kang Youl Bae*, Chung Seob Yi*, Jae Ho Shin*, Hyo Min Jeong* and Han Shik Chung***

*Department of Transport Vehicle Engineering, Gyeongsang National University
445, Inpyeong-dong, Tongyoung, Kyongnam, 650-160, Korea

**ABSTRACT** The natural convective heat transfer in a rectangular enclosure with a heating source point has been studied by experiment and numerical analysis. The governing equations were solved by a finite volume method, a SIMPLE algorithm was adopted to solve a pressure term. The parameters for the numerical study are positions and surface temperatures of a heating source point i.e., Y/H=0.25, 0.5 0.75 and 11℃≤Δ T≤59℃. The results of isotherms and velocity vectors have been represented, and the numerical results had a good agreement with experimental values. Based on the numerical results, the mean Nusselt number of the rectangular enclosure wall could be expressed as a function of Grashof number.

**Keywords:** Heating source, Low Reynolds Number, Turbulence Model, Nusselt Number, Grashof Number

## 1. INTRODUCTION

The heat transfer in rectangular space with heating source point has been applied to industrial problems. These researches are very important to the radiative heat control in PCB(Printed Circuit Board), solar collector, accumulator and ship equipments, and they can change the machinery performances. Thus, there are many kinds of calculation methods for basic or optimum design, and the natural convective heat transfer is very popular to understand the heat transfer mechanism or flow characteristics inducing the temperature differences[1]-[6]. Many of authors suggested the numerical model to calculate the turbulent natural convection in enclosure space, and it is well known that the low Reynolds number model have a good agreements with an experimental results[7]-[9].

In this paper, we compared with the experimental results for selecting the most useful low Reynolds number turbulence model. Fig. 1 represents the comparison with Cheesewright's experimental results and three types of a low Reynolds number turbulence model, and this contains vertical velocity and turbulent kinetic energy distributions at Y=1.25m and temperature distribution at X=0.25m. In this figure, ST, LS and DA mean a standard k-ε turbulence model, low Reynolds number turbulence model by Launder-Sharma and Davison respectively. As these comparisons, the ST model showed an excessive velocity, temperature and turbulent kinetic energy, and this means the wall boundary condition is very important. But the two LS and DA models had a good agreement with experimental results at whole section. Especially, the LS model was excellent near the wall[10]-[11].

In this paper, we perform a numerical simulation of natural convection in a rectangular enclosure by using the LS

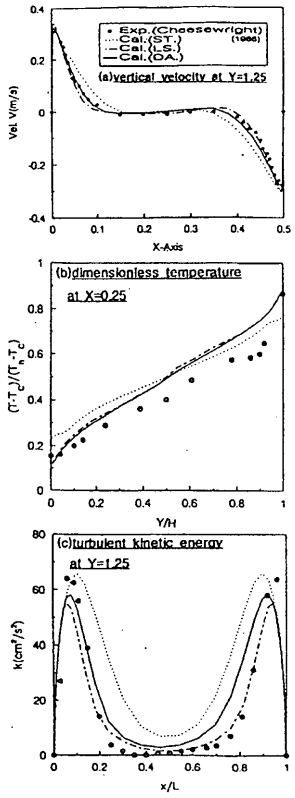


Fig. 1 Comparisons of a numerical analysis with a several turbulence models and Cheesewright's experimental results(1986) for L×H=0.5×2.5(m).

turbulence model, and the results are compared with the experimental data by holographic interferometer.

## 2. NUMERICAL SIMULATION

### 2.1 Governing Equations

Figure. 2 shows the numerical model with L × H=0.04 × 0.12(m). We traversed the three type of the heating source position, Y=0.03m, 0.06m, and 0.09m, the top and bottom wall is adiabatic, left and right wall is cooling at constant temperature, Tc=0℃. We introduced the LS model by Launder and Sharma, and the governing equations are as follows:

Continuity

$$\frac{\partial(\rho U_i)}{\partial X_i} = 0 \tag{1}$$

Momentum

$$\frac{\partial(\rho U_i U_j)}{\partial X_j} = -\frac{\partial P}{\partial X_i} + \frac{\partial}{\partial X_j}\left[\mu\left(\frac{\partial U_i}{\partial X_j}\right) + \left(\frac{\partial U_j}{\partial X_i}\right)\right] - \frac{\partial}{\partial X_j}\left[\rho\overline{u_i u_j}\right] + \delta_{i2}\rho g\beta\Delta T \tag{2}$$

Energy

$$\frac{\partial(\rho U_j T)}{\partial X_j} = \frac{\partial}{\partial X_j}\left[\left(\frac{\mu}{P_r} + \frac{\mu_t}{\sigma_t}\right)\frac{\partial T}{\partial X_j}\right] \tag{3}$$

Turbulent kinetic energy

$$\frac{\partial(\rho U_j k)}{\partial X_j} = \frac{\partial}{\partial X_j}\left[\left(\frac{\mu_t}{\sigma_k} + \mu\right)\frac{\partial k}{\partial X_j}\right] + G - \rho\varepsilon + B - 2\mu\left(\frac{\partial\sqrt{k}}{\partial X_j}\right)^2 \tag{4}$$

Dissipation rate

$$\frac{\partial(\rho U_j \varepsilon)}{\partial X_j} = \frac{\partial}{\partial X_j}\left[\left(\frac{\mu_t}{\sigma_\varepsilon} + \mu\right)\frac{\partial \varepsilon}{\partial X_j}\right] + C_{1\varepsilon}\frac{\varepsilon}{k}(G + B) - C_{2\varepsilon} f_2 \frac{\rho\varepsilon^2}{k} + 2\frac{\mu\mu_t}{\rho}\left(\frac{\partial^2 U_i}{\partial X_j \partial X_k}\right) \tag{5}$$

where G and B are the turbulent generation term and the buoyancy term, respectively:

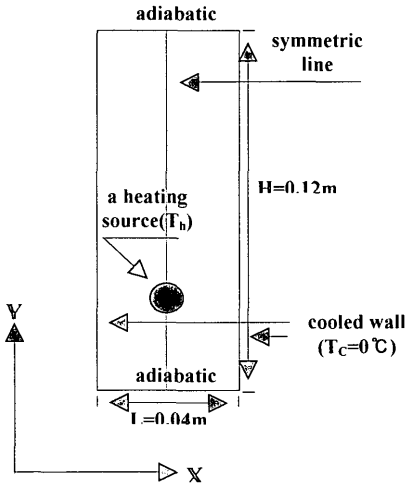


Fig. 2 Schematic diagram for rectangular enclosure with a heating source.

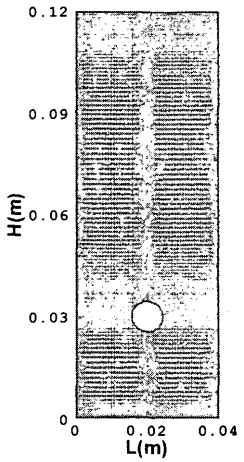


Fig. 3 Grid generation system.

$$G = \mu_t\left(\frac{\partial U_i}{\partial X_j} + \frac{\partial U_j}{\partial X_i}\right)\frac{\partial U_i}{\partial X_j}$$

$$B = -g\beta\frac{\mu_t}{\sigma_t}\frac{\partial T}{\partial y} \tag{6}$$

Here, the turbulence model constants and functions are given as follows:

$$C_{1\varepsilon}=1.44,\ C_{2\varepsilon}=1.92,\ \sigma_\varepsilon=1.3,\ \sigma_k=1.0,\ C_\mu=0.09,\ \sigma_t=0.9$$

$$f_2 = 1 - 0.3\exp(-R_{et}^2),\ f_\mu = \exp\left\{\frac{-3.4}{(1+R_{et}/50)^2}\right\}$$

$$R_{et} = \frac{\rho k^2}{\mu\varepsilon},\ \mu_t = \frac{f_\mu C_\mu \rho k^2}{\varepsilon} \tag{7}$$

In this study, we adopted finite volume method for solving each values from given equations, SIMPLE algorithm was used to solve a pressure term.

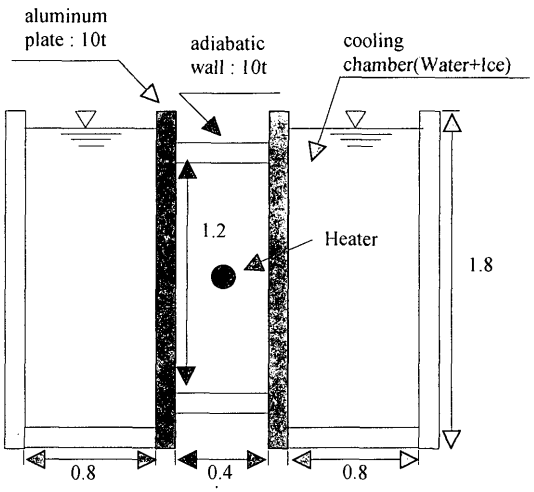


Fig. 4 Experimental apparatus of rectangular enclosure with a heating source.

Fig. 3 shows a grid system for numerical analysis, and adopted a non-constant grid by using equation(8) for dense arrangement near a heat source and the wall side.

$$X_i = X_{\max}\left[-0.5\tanh\left\{a(2\frac{i}{n-1})/\tanh(-a)+0.5\right\}\right] \quad (8)$$

where $n$ is grid number of X-direction. The $i$ is coordinate position and $a$ is a coefficient for adjusting the grid interval. The diameter of a heating source is 0.008m.

### 2.2 Experimental Methods

Fig. 4 shows the experimental apparatus. The experimental test section is rectangular enclosure with $0.04 \times 0.12 \times 0.4$(m). The heating source is traversed to vertical direction at symmetric line of rectangular space. The left and right wall is adjacent to cooling chambers with 0℃ temperatures, it is preserved by mixturing a ice, salt and water. The temperature measurement was conducted by using T-type thermocouple, hybrid recorder and P/C, and a holographic interferometer was used for visualization as shown in Fig. 5 and Fig. 6.

## 3. RESULTS & DISCUSSION

Fig. 7, Fig. 8 and Fig. 9 show comparisons with experimental and numerical isotherms according to the position of a heating source.

Fig. 7 represents the experimental photograph and the numerical result when the a heating source is on the lower position for various temperature differences(20, 32 and 47℃). Generally, the density of isotherms was great around the heating source, and these were more dense at the upper space than the lower space. Because the air is expanded to the upper space by heating. As $\Delta T$ is great, the isotherms

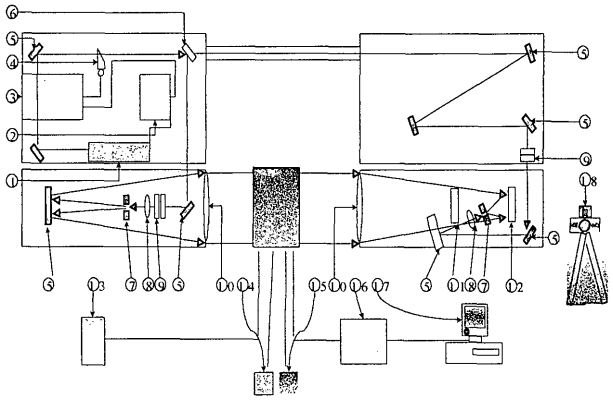

(1)He-Ne Laser (2)He-Ne Laser Power Supply (3)Shutter Controller
(4)Shutter (5)Mirror (6)Beam splitter
(7)Spatial Filter (8)Objective (9)PL Filter
(10)Field Lens (11)Circular (12)Holographic Plate Holder
(13)AVR (14)Voltage Meter (15)Current Meter
(16)Data Logger (17)PC (18)Camera (19)Test Section

Fig. 5 Schematic diagram of Holographic Interferometer.

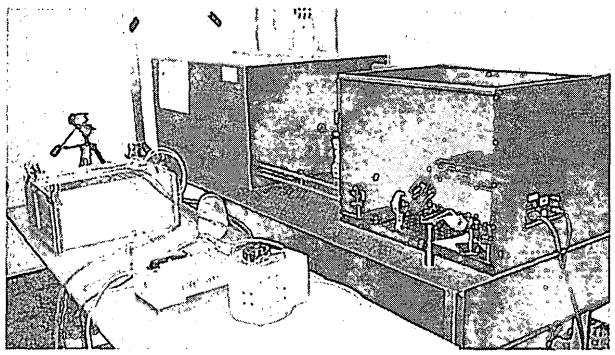

Fig. 6 The photograph of Holographic Interferometer.

were more dense, and the numerical results showed a good agreements with experiment.

Fig. 8 shows results for the center position, and the temperature distributions were very similar to the above case, but it was more dense near the ceiling.

Fig. 9 shows isotherms distributions for upper position of a heating source. The isotherms were very dense at upper side and near the ceiling.

Fig. 10 shows velocity vectors for various the positions of a heating source at $\Delta T$=20℃. The magnitudes of the velocity vectors were very small at the lower space of a heating source, but the velocity vectors were very large at the center and side wall; one is up-flow by the buoyancy of hot fluid and the other is down-flow by side cooling walls.

Fig. 11 and Fig. 12 show distributions of velocity at $\Delta T$=32℃ and 47℃, respectively, all of these velocity vectors were very similar, but the magnitude of vectors were increased as increasing the temperature of difference.

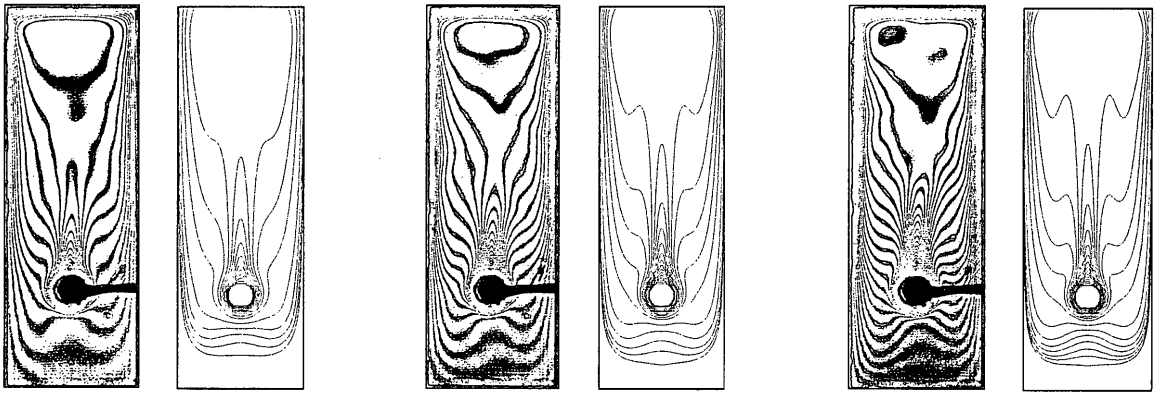

(a) ΔT=20°C (b) ΔT=32°C (c) ΔT=47°C

Fig. 7 Comparison with experimental and numerical isotherms for various ΔT (lower position)

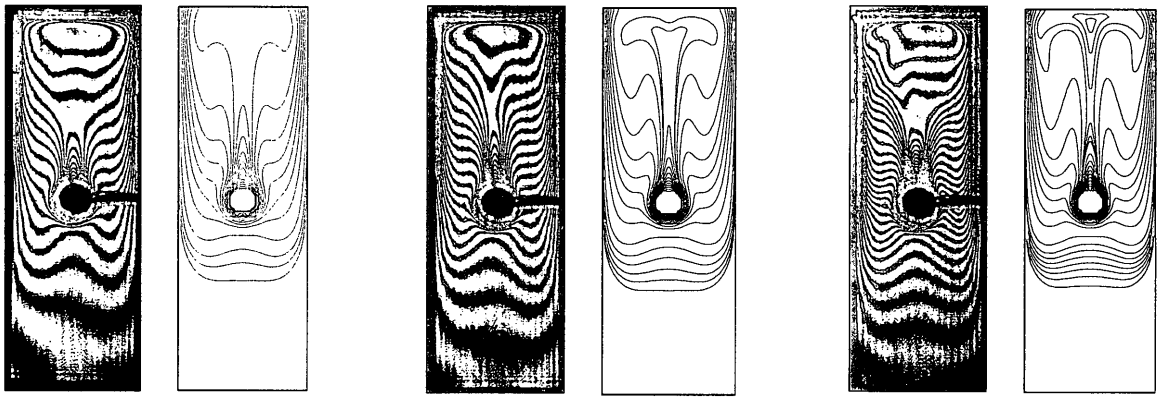

(a) ΔT=20°C (b) ΔT=32°C (c) ΔT=47°C

Fig. 8 Comparison with experimental and numerical isotherms for various ΔT (center position)

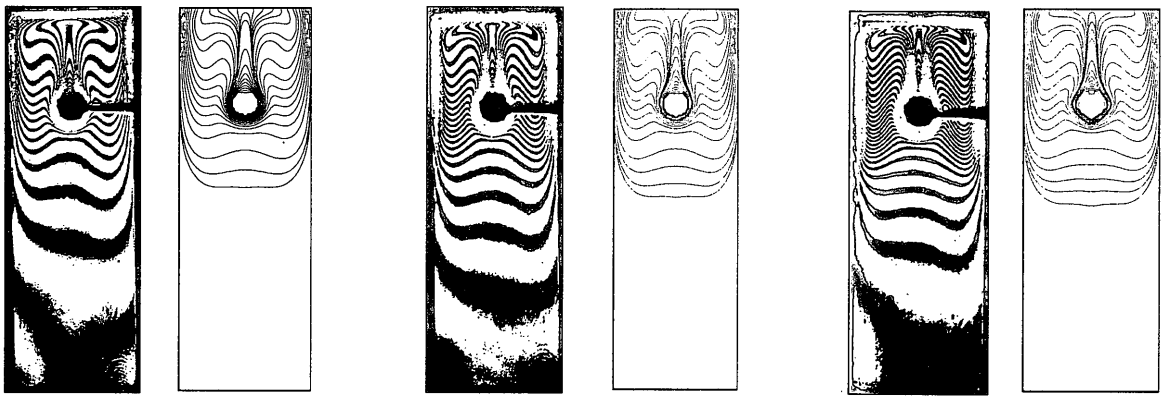

(a) ΔT=20°C (b) ΔT=32°C (c) ΔT=47°C

Fig. 9 Comparison with experimental and numerical isotherms for various ΔT (upper position)

Fig. 13 represents Nusselt number distributions on the side vertical wall with the position of a heating source. The Nusselt number was very small at the lower wall and large at the upper wall from the heating source.

The gradient of the Nusselt number was zero at Y/H≒0.9, this means that there is a stagnation region at near the ceiling. Fig. 14 represents a distribution of vertical wall's mean Nusselt number versus Grashof number for various positions of a heating source. The mean Nusselt number is increased proportionally to the Grashof number, the heat transfer at Y/H=0.5 was greater than other cases. Also, the relationships between the mean Nusselt number and Grashof number on each position could be obtained, and the correlation equations are as follows:

at lower position

$$\overline{Nu.} = 1.6895 + 6.2924 \times 10^{-8} Gr.$$

at center position

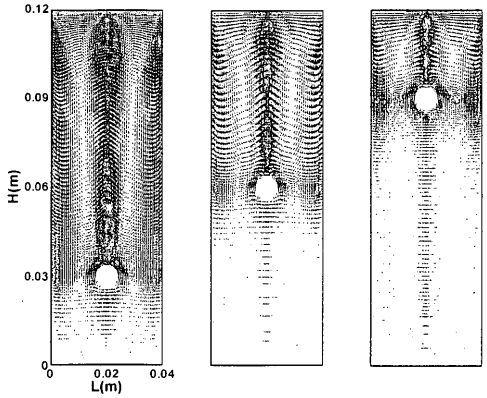


(a) lower (b) center (c) upper

Fig. 10 Velocity vector on various positions at ΔT=20°C

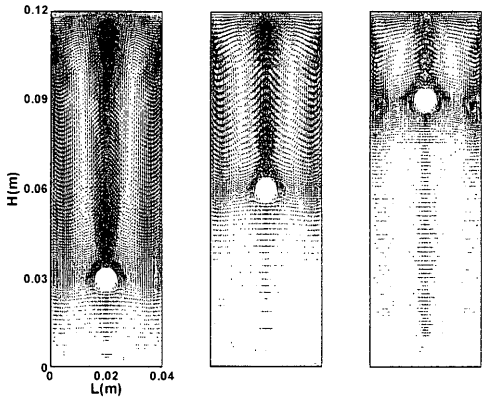


(a) lower (b) center (c) upper

Fig. 11 Velocity vector on various positions at ΔT=32°C

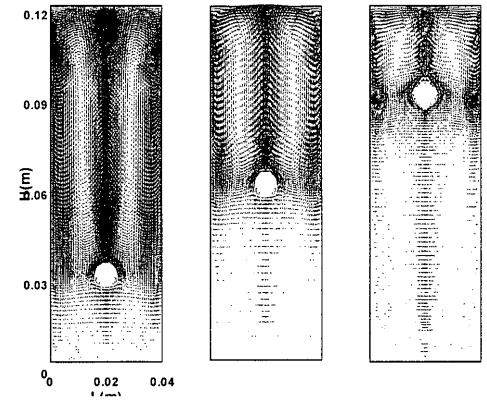


(a) lower (b) center (c) upper

Fig. 12 Velocity vector on various positions at ΔT=47°C

$$\overline{Nu.} = 1.5704 + 1.0411 \times 10^{-8} Gr.$$

at upper position

$$\overline{Nu.} = 1.6725 + 3.2642 \times 10^{-8} Gr. \quad (9)$$

## 4. CONCLUSIONS

The results of numerical analysis gave a good agreement with the experiment.

1. The isotherm distributions of numerical analysis and

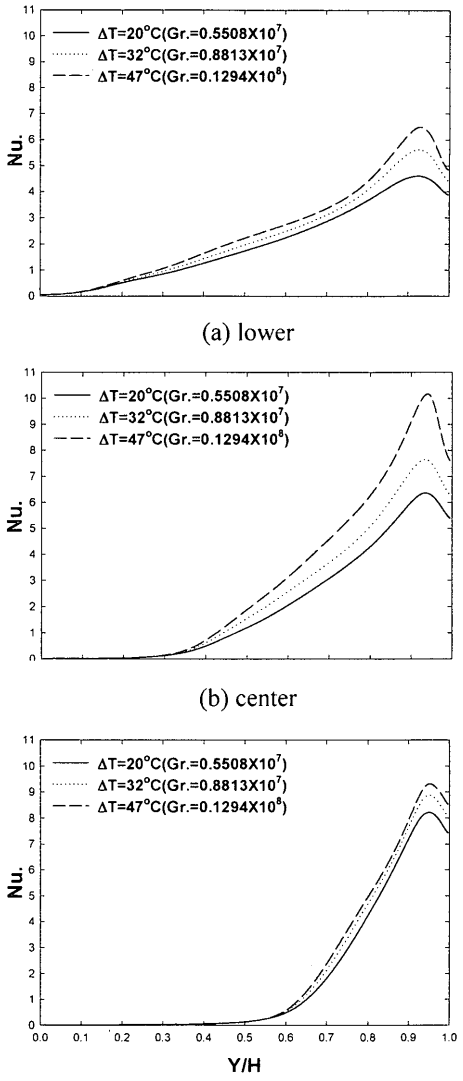


(a) lower

(b) center

(c) upper

Fig. 13 Nusselt number distributions on vertical wall for various heating positions by the numerical analysis.

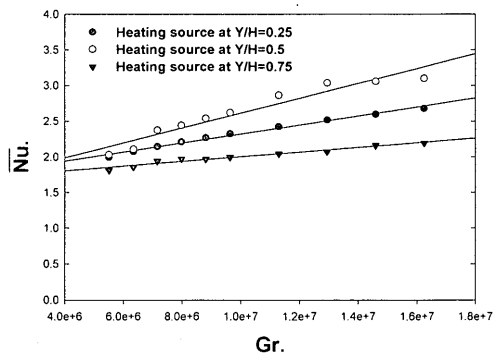


Fig. 14 Distributions of Nusselt number vs. Grashof number with each position by the numerical analysis.

experimentation shows the qualitative same, and as the temperature increases, the dense isotherm is appeared.
2. The lower space of a heating source had very small velocity vectors, and temperature was very low, thus, as increasing the temperature differences, the isotherms were dense at the center and wall.
3. The local Nusselt number on the side wall was increased according to the vertical wall, and the gradient of Nusselt number was zero at Y/H≒0.9.
4. The relationships between the mean Nusselt number and Grashof number were obtained linearly.

## 5. REFERENCE


1. H. M. Jeong, C. J. Lee, H. S. Chung, Study on the Numerical Modeling of Turbulent Natural Convection in Rectangular Enclosure, Journal of SAREK, Vol. 10, No. 2, (2000), pp.33-39.
2. J. H. Lee, M. H. Kim, J. H. Moh, Natural Convection Heat Transfer in Rectangular Air Enclosure with Adiabatic and Isothermal Horizontal Boundary Condition, Journal of KSME, Vol. 14, No. 1, (1990), pp.207-213.
3. D. K. Kang, W. S. Kim, K. S. Lee, A Numerical Study on the Two- Dimensional Turbulent Natural Convection Using a Low-Reynolds Number k-$\varepsilon$ Model, Journal of KSME, Vol. 19 No. 3, (1995), pp.741-750.
4. Suhas V. Patankar, Numerical Heat Transfer and Fluid Flow, (1980).
5. H. S. Chung, H. M. Jeong, K. K. Kim, S. T. Ro, The Turbulent Natural Convection in Membrane Type LNG Carrier Cofferdam, Journal of KSME, Part B, Vol. 23, No. 2, (1999), pp.281-287.
6. R. Cheesewright, K. J. King, and S. Ziai, Experimental data of the Validation of Computer Codes for the Prediction of Two Dimensional Buoyancy Cavity Flow, Significant Questions in Buoyancy Affected Enclosure or Cavity Flows, ASME-HTD, (1986), pp.75-81.
7. T. G. Kim, H. J. Sung, A Hybrid Turbulence Model for Prediction of Buoyancy-Driven Turbulent Thermal Convection Flow, Journal of KSME, Vol. 17, No. 8, (1993), pp.2069-2078.
8. H. T. Seo, D. S. Lee, S. H. Yoon, J. S. Boo, Numerical Analysis on Wall-Attaching Offset Jet with Various Turbulent k-$\varepsilon$ Models and Upwind Scheme, Journal of KSME, Part B, (1998), pp.828-835.
9. Kumar. K, Mathematical Modeling of Natural Convection in Fire-a State of the Art Review of the Field Modeling of Variable Density Turbulent Flow, Fire and Materials, Vol.103, (1983), pp.456-460.
10. C. J. Lee, H. M. Jeong, H. S. Chung, K. K. Kim, Study on the Natural Convection of Rectangular Enclosure with Heating Source, Proceeding of KSME, Part B, (1998), pp.417-421.
11. W. Shyy and M. M. Rao, Simulation of Transient Natural Convection Around an Enclosed Vertical Channel, Journal of Heat Transfer, the ASME, Vol.115, (1993), pp.946-954.


## ACKNOWLEDGEMENTS

This work was supported by Korea Maritime Institute and the Brain Korea 21 Projects, and the authors gratefully appreciate the support.

## NOMENCLATURE

a : grid space regulation coefficient
g : gravity acceleration[m/s$^2$]
Gr. : Grashof number ($Gr = \frac{g\beta(T_h - T_c)H^3}{\nu^2}$)
H : vertical wall length[m]
$k$ : turbulent energy[m$^2$/s$^2$]
L : horizontal wall length[m]
Nu. : local Nusselt number ($Nu = \frac{hL}{k} = -\frac{\partial\theta}{\partial X}|_{X=0}$)
$\overline{\text{Nu}}$ .: mean Nusselt number ($\overline{Nu} = \frac{1}{L}\int Nu \cdot dy$)
Pr : Prandtl number
T : temperature[°C]
$T_h$ : heating source temperature[°C]
$T_c$ : cooled wall temperature[°C]
U : X direction velocity[m/s]
V : Y direction velocity[m/s]
$\beta$ : thermal expansion coefficient[K$^{-1}$]
$\delta_{ij}$ : Kronecker delta
$\varepsilon$ : turbulent energy dissipation rate
$\mu_t$ : turbulent eddy viscosity[kg/ms]
$\rho$ : density[kg/m$^3$]